ORNL Oxygen Broomstick Experiment: MCNP model and evaluation results for SINBAD entry NEA-1517/59

S. Simakov[1], U. Fischer[1]

[1] Institute for Neutron Physics and Reactor Technology

Institut für Neutronenphysik und Reaktortechnik
Hermann-von-Helmholtz-Platz 1
76344 Eggenstein-Leopoldshafen
www.inr.kit.edu

ORNL Oxygen Broomstick Experiment: MCNP model and evaluation results for SINBAD entry NEA-1517/59.

S. Simakov and U. Fischer

Karlsruhe Institute of Technology

Institute for Neutron Physics and Reactor Technology

Hermann-von-Helmholtz-Platz 1, 76344 Eggenstein-Leopoldshafen, Germany

Abstract

The existing entry NEA-1517/59 (SDT2) of the SINBAD database comprises the results of measurement of the neutron transmission spectra through the liquid oxygen broomstick of the length 60" (152.4 cm). The experiment was performed in 1965 at the Tower Shielding Facility located in Oak Ridge National Laboratory and was designed to measure the neutron total cross sections in the range of 1.9 – 8.6 MeV. The purpose of the present work was to assemble the MCNP input deck for the Monte Carlo code MCNP, perform the sample calculations of the radiation transport and sensitivities with evaluated neutron reaction cross section from ENDF/B-VIII.0 and JEFF-3.3, to show the impact on the (n,tot) and (n,α) cross sections and thus to demonstrate the value of this benchmark for the validation of the modern evaluated data. The impact of validation benchmark on $^{16}O(n,\alpha_0)$ cross section was shown do agree with the thick target neutron yield induced by α-particles with energies up to 5 - 6 MeV in carbon. An attempt was also made to find the missing measured data for other ORNL O-broomsticks of length 24" (60.96 cm), 36" (91.44 cm) and probably 72" (182.88 cm).

November 2022

Content

Introduction

The evaluated cross section data files require a validation against the experimental benchmarks. To facilitate this, the compilation of detailed experimental results and input decks for the radiation transport code simulations in the Shielding Integral Benchmark Archive and Database (SINBAD) [1] or International Criticality Safety Benchmark Evaluation Project (ICSBEP) [2] is a valuable task. Such goal was considered by dedicated subgroup 47 (SG47) "Use of Shielding Integral Benchmark Archive and Database for Nuclear Data Validation" of the Working Party on International Nuclear Data Evaluation Co-operation (WPEC) under auspicious of the Nuclear Energy Agency (NEA) in Paris during time period 2019 – 2021 [3], in which the authors participated.

The neutron transmission through the liquid oxygen broomsticks was measured at the Tower Shielding Facility (TSF) operated by Oak Ridge National Laboratory (ORNL) around 1967 - 1968 [4 - 8]. The data for the 60" (152.4 cm) long broomstick were already compiled in the SINBAD database under entry NEA-1517/43 (SDT2) [9]. Besides the oxygen the deep neutron penetration for several other materials were measured at this facility and are available in SINBAD [10]. These experiments were designed in the pin neutron beam geometry to minimize the fraction of collided neutrons and thus to be most sensitive to minima in the total neutron cross section. The set-up configuration and large sample thickness in range of several neutron mean free paths (mfp) have allowed the authors to use the simple analytical approach, namely the uncollided transmission, to validate existing at that time the cross sections in the energy range from 1 to 8 MeV.

The present work reports a creation of the input deck for the ORNL O-broomstick experiment to be used with the MCNP code [11]. It also includes the benchmarking results for the ENDF/B-VIII.0 [12] and JFFF-3.3 [13] libraries and sensitivity analysis. The evaluated data were processed in the ACE format by the NJOY21 code [14]. The disagreement observed for benchmark was propagated on the microscopic oxygen total and alpha production cross sections. The impact of the ORNL 60" O-broomstick on $^{16}O(n,\alpha)^{13}C$ was cross-checked by the measured thick carbon target (α,n) yields. Report and MCNP input deck will be included in the updated entry NEA-1517/43.

The preliminary results were presented at several meetings of Subgroup 47 "Use of Shielding Integral Benchmark Archive and Database for Nuclear Data Validation" of WPEC [15 - 17].

1. Description of the ORNL Oxygen Broomstick Experiment

This section summarise the details of the experiment needed for the MCNP deck creation and Monte Carlo simulation. The complete description of experiment is available in the original publications [4 - 8] and in the SINBAD entry NEA-1517/43 (SDT2) [9]. The experimental arrangement is shown in Fig. 1.1. To achieve the maximum ratio of uncollided and collided fluxes the detector and source were located at large distance 100 feet (30.48 m), the long thin sample was positioned in between, the incident and transmitted neutron beams were thoroughly collimated.

A source of neutrons was the Tower Shielding Reactor TSR-II, sketched in Fig. 1.1. The cylindrical exit channel in the shield (water mixed with lead) of the reactor core had stepped diameters 10 – 15 inches followed by two water and lithiated paraffin collimators with minimal aperture 2¾". They formed a pin beam of the neutrons incident on the broomstick.

The liquid oxygen was contained in Dewar vessels having diameter 4" (10.16 cm) and lengths 24" (60.96 cm) and 36" (91.44 cm). The containers altered the shape of the energy spectrum of neutron incident on the sample by less than 5%. The longest sample 60" (152.4 cm) was obviously assembled from two smaller ones [5]. Commercial liquid oxygen with 99.9% content of O_2 was used in this experiment. To reduce the air and ground scattering effects, the neutron beam emerging from reactor was additionally collimated to diameter of 3½" (8.89 cm) by the water collimator located just before the sample.

The energy spectra of transmitted neutrons were measured NE-213 scintillation detector having diameter 1.88" (4.7752 cm) and length 1.99" (5.0546 cm). It was surrounded by 14" thick layer of lead and 15" of water which had a cylinder hole of Ø3" looking on the sample. For better collimation an additional water tank with 3¼" hole was positioned in front of shielded neutron detector. It is important to cite following note from Report ORNL-TM-3868 (Revised) [7]: *"Throughout of this experiment, a 2-in.-thick sample of lead, not pictured in Fig. 1, was placed in the beam to reduce the gamma-ray intensity incident on the NE-213."*
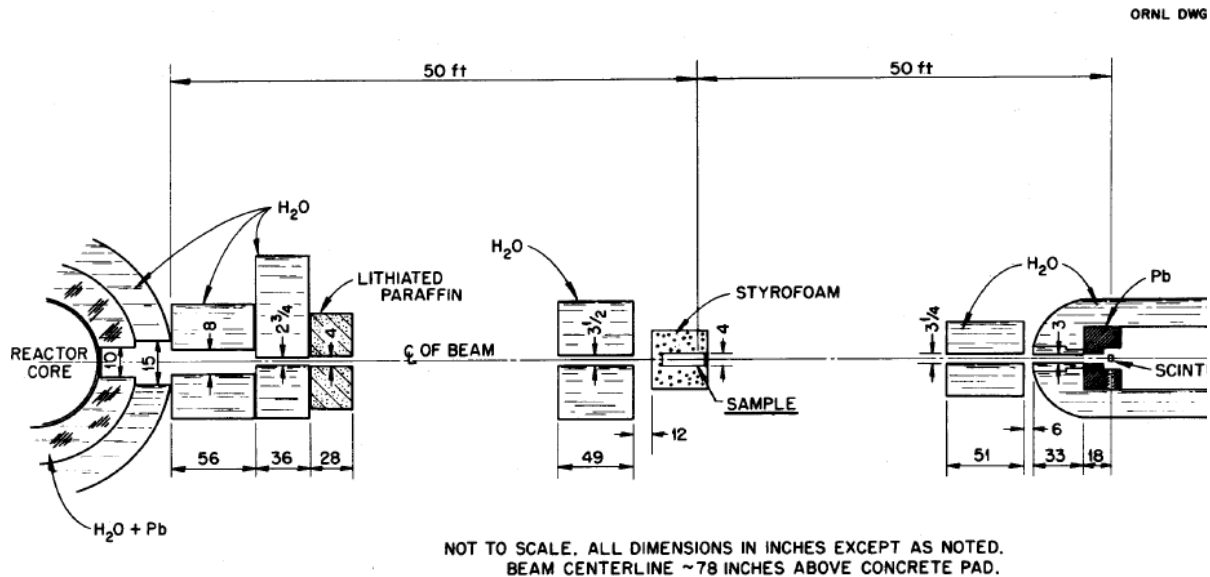

Fig. 1.1. The ORNL arrangement at Tower Shielding facility with TSR-II reactor to measure the neutron spectra transmitted through the thick samples. Figure is copied from Report ORNL-2242 [5].

The sensitivity of the NE-213 detector to γ-rays was supressed with the help of neutron- and gamma-induced pulses discrimination circuit. The pulse-height distribution of recoils in NE-213 scintillator was converted into the neutron energy spectrum by unfolding procedure. The response functions was obtained from Monte-Carlo simulations and checked by several calibration experiments. The neutron spectra were reported in the energy range 1.9 to 8.6 MeV.

The room returned background was measured with a shadow bar manufactured from 28" long water cylinder in the aluminium tube of Ø4" followed by 4" thick lead cylinder. This shadow bar replaced the oxygen broomstick.

The spectrum of neutrons incident on sample (i.e., from TSR-II) was measured by the same NE-213 detector at the same location but with emptied Dewar vessel and with 4" lead in place. This spectrum is tabulated in Report ORNL-TM-3868 (Revised in Sep 1972) [7] and is plotted in Fig. 1.2.

The authors of this report additionally investigated the effect of the possible fine structure in the source beam on the ca1cu1ated uncollided spectrum [7]: *"The materials through which the source beam had penetrated ... was approximately 2 in. of water, 3 1/2 in. of aluminium, 4 in. of lead, 1/4 in. of iron, and the empty Dewars. By ca1culating the uncollided flux through these materials, smoothing with the NE-213 reso1ution function, and normalizing to the measured source spectrum, a structured normalized source spectrum was obtained. This structured source was then attenuated through the liquid oxygen and smoothed. Since oxygen occurs in the water, a selective fine structure in the source beam can be expected to resu1t in the sense that the neutrons transmitted through the water in the immediate vicinity of the oxygen total cross section minima are somewhat greater, and off the minima somewhat 1ess, than*

3

the poor reso1ution NE-213 source measurement would indicate. Such indeed has been found to be the case, and a table of approximate correction factors that should be used to mu1tip1y the results ca1culated on page 13 appears on Addendum #2."
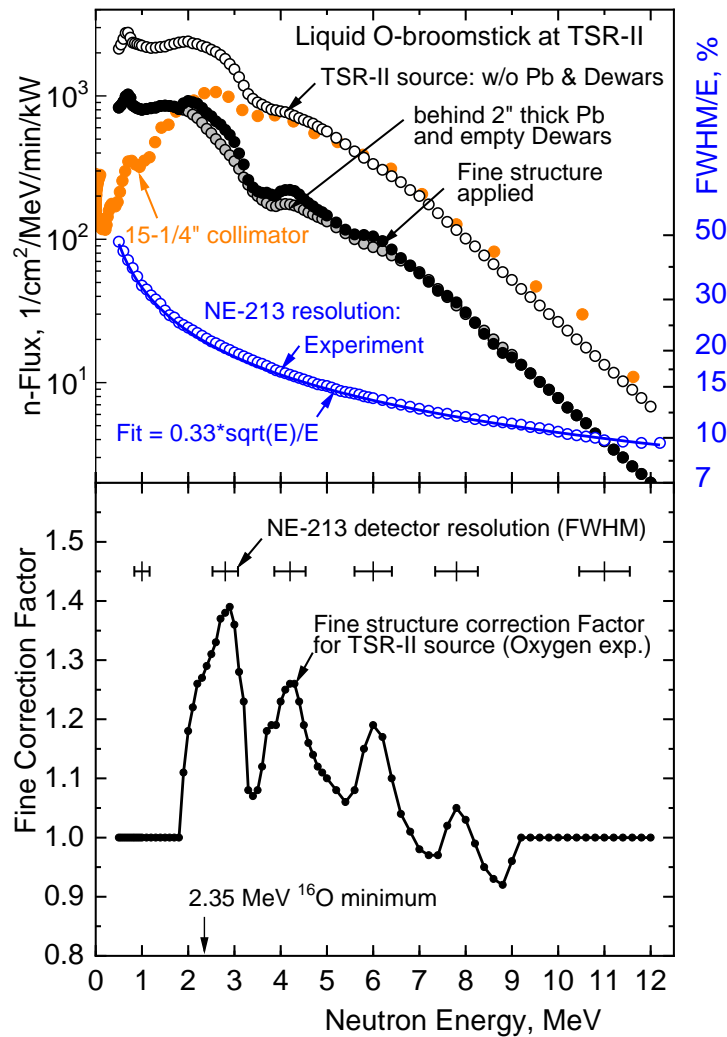

Fig. 1.2. Top: the TSR-II source energy spectra measured by NE-213 detector with the empty Dewar vessel and 2" lead in place (data from Report ORNL-TM-3868 (Revised 1972) [7], open circles) and without them (data from Report ORNL-TM-3867 (Revised 1972) [20], close circle); behind 15-¼" collimator at point A shown in Fig. 1.3 (data are from Report ORNL-TM-4010 [8], orange circles). Relative energy resolution of NE-213 detector: experimental data from [7] (blue symbol) and fit we used in MCNP deck (blue curve). Bottom: correction factors for calculated spectrum to account for the fine structure in source beam (data from [7]), the NE-213 detector energy resolution (FWHM) is plotted by horizontal bars.

The correction function from Report ORNL-TM-3868 (Revised 1972) [7] is plotted in Fig. 1.2 together with the energy resolution of the NE-213 detector taken from the same report. The amplitude of the calculated fine correction for neutron beam transmitted through the ≈ 5" (12.7 cm) thick layer of the water shield around the TSR-II core reaches 40%. To increase the reliability of the present benchmark, the transmission of the core fast neutrons through the water shield could be nowadays re-simulated with higher precision and contemporary data. As an example, we refer to the recently precisely calculation of the similar correction for the $^{235}U(n,f)$ fission spectrum behind the ≈ 5 cm water layer in VR-1 reactor caused by the O(n,tot) resonances and H(n,tot) cross section [18].

For comparison, the TSR-II source spectrum measured behind 15-¼" collimator at point A shown in Fig. 1.3 and reported in ORNL-TM-3867 (Revised 1972) [20] is also plotted. As seen, the TSR-II spectrum essentially depends on the exit hole and collimator configurations below ≈ 3 MeV.
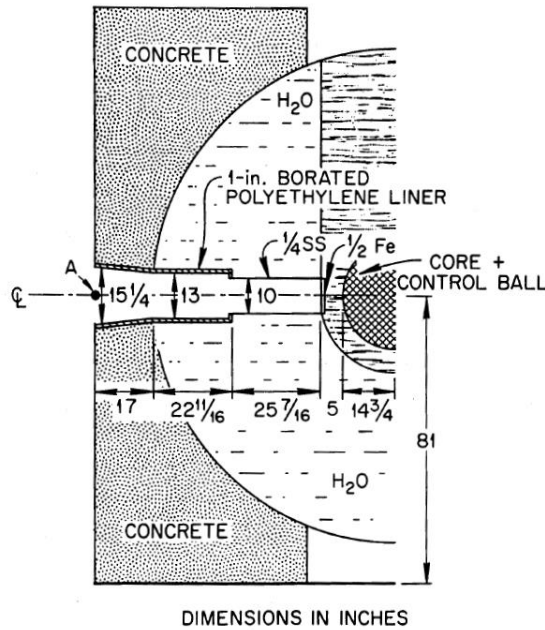
Fig. 1.3. Diagram of the 15¼" collimator arrangement for the TSR-II reactor of the Tower Shielding Facility. The sizes are given in inches. Figures are copied from Report ORNL-TM-4010 [4] (top) and ORNL-TM-4592 [19] (bottom).

The spectrum of neutrons transmitted through the 60" (152.4 cm) oxygen broomstick is available in the SINBAD database. Regrettably but the data for another two O-broomsticks of length 24" (60.96 cm) and 36" (91.44 cm) are not compiled (the spectra were indeed measured, since they are plotted in Figs. 7

5

and 8 of paper [4]). Probably, the transmission through 72" (182.88 cm) long liquid oxygen broomstick was also measured since it is listed in Report ORNL-4134 [6]. One of the authors (S.S.) of present report communicated with RSICC at ORNL but did not get any measured data for the missing broomstick thicknesses.

The numerical data for the uncollided transmitted spectra through 60" thick liquid oxygen were presented as upper and lower 68% confidential limits after re-unfolding of the original NE-213 spectrometer results utilizing code FERDoR [21]. They are plotted as up- and down-triangles in Fig. 1.4. We consider their arithmetic average and deviations of upper and lower limits as a transmitted spectrum N(E) and its statistical uncertainties, correspondingly. The upper limit ±10%, given as an error in the absolute spectrum due to power calibration uncertainties, we accepted as the spectrum systematic uncertainty.
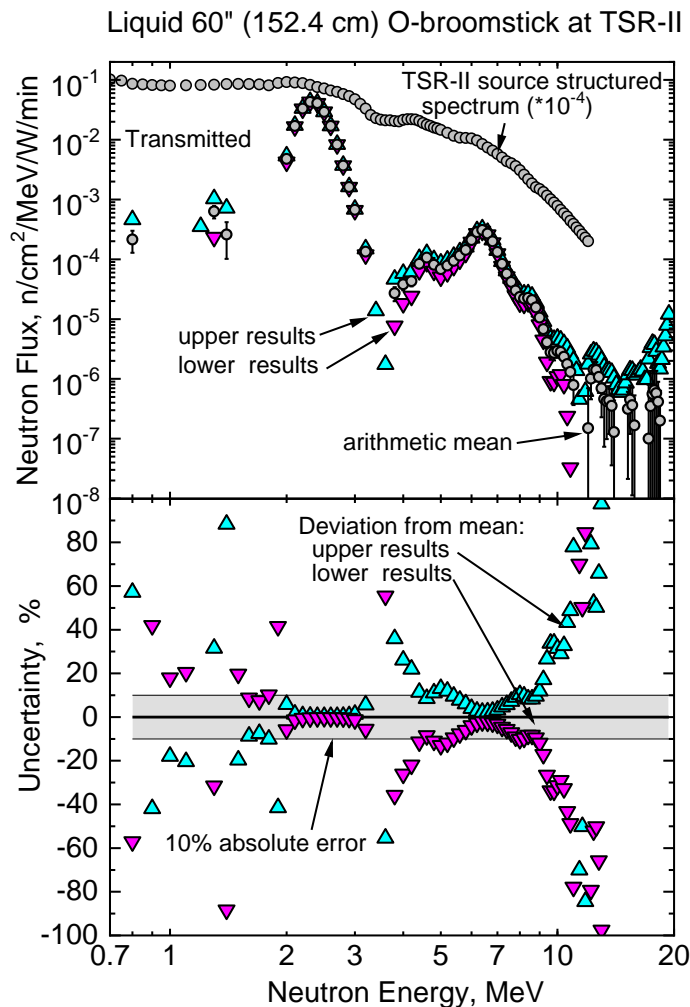
Fig. 1.4. Top: the energy spectra of neutrons from the TSR-II source (circles) and transmitted through the 60" O-broomstick measured at ORNL (data from [7] and NEA-1517/59 [9]): up/down triangles – upper/lower 68% confidence limits for the unfolded spectrum, circles - arithmetic average. Bottom: the deviation of upper and lower data from arithmetic mean (up and down triangles) and ±10% uncertainty for absolute normalization (grey corridor).

I

t has to be noted that some tabulated values of the upper and lower limits of the 60" broomstick spectrum are negative, consequently the averaged spectrum is less than zero at several energies. Moreover, as seen in Fig. 1.4, the scattering around the average exceeds 50% above 10 MeV. To work with reliable data, we limited the usage the measured uncollided spectrum N(E) to the energy intervals 2.0 to 3.2 MeV and 3.8 to 8.0 MeV.

2. MCNP input deck assembled for the ORNL oxygen broomstick

This section describes the input deck of the ORNL oxygen broomstick benchmark which was created and included in the present SINBAD entry. The main features, which are substantial for computing of the relevant responses and nuclear data benchmarking, are presented in this section. Other details are available in the input deck as self-explaining comments.

Fig. 2.1 displays and explains the geometry of the MCNP model for the ORNL experiment. The center of the (X,Y,Z) coordinate system is located in the middle point of the cylinder oxygen broomstick of 4" (10.16 cm) diameter and 60" (152.4 cm) length. The sample axis and neutron beam direction coincide with Z axis. The neutron detector, Ø2 × 2" cylinder, was positioned at distance 50 feet (600" = 1524.0 cm) from broomstick center.

Fig. 2.1. The MCNP model for the ORNL O-broomstick transmission experiment with TSR-II as a neutron source. Top: an overall geometry and sizes with superimposed conical beam of incident neutrons (green); neutrons start at rear surface of the Ø2¾" water collimator. Bottom: plot from MCNP showing the O-broomstick Ø4"×60" (pink cell #2) and the source neutron beam (within the conical surface #1).

The key feature of the proposed geometrical model for the Monte-Carlo simulation is following: the nearly parallel pin-like neutron beam hits only the part of the front surface of sample, the neutrons passed through the broomstick are observed by the neutron detector located far behind the sample. To realise this geometry the neutron beam incident on sample was restricted by the cone, one of its base coincides with exit plane of the first H₂O collimator of diameter 2¾" (6.985 cm) and other - with the exit plane of second H₂O collimator of diameter 3½" (8.890 cm). The bottom part of Fig. 2.1 depicts this

configuration and visually proves that the selected apertures are the most narrow ones and do form the neutron beam.

The opening angle of the beam cone is equal 0.0461071 degree. The radius of the neutron spot even on the rear surface of the Ø4" (radius 5.080 cm) × 60" oxygen broomstick is 4.506 cm, thus assuring that every TSR-II source neutron passes through the entire thickness of the sample. The radius of the neutron spot on the NE-213 detector middle surface (located at 50 ft or 1524 cm) is 5.671 cm, assuring that the whole detector is within neutron source beam. The mean angle subtended by Ø4"×60" oxygen broomstick from view of detector is 0.190985 degree. The latter is 4 times as large as divergence of incident beam and thus defines the angular resolution of this experiment.

The TSR-II reactor source of neutrons in the ORNL experiment in the MCNP deck was modelled with the SDEF and several distribution cards. The neutrons start at the spherical surface segment restricted by the beam cone and fly away in normal direction. The part of MCNP geometry model shown in Fig. 2.1 confirms that the source neutron beam, when it hits the broomstick, has diameter smaller than 4 inches.

The energy distribution of the source neutrons was measured by the authors of experiment [7] with by the same NE-213 detector but when the O-broomstick was replaced by empty Dewar vessels. The impact of materials through which the reactor neutrons penetrated (approximately 2" of water, 3½" of aluminium, 4" of lead, ¼" iron, and the empty Dewar) was studied by authors and represented as tabulated approximate correction factors, Fig. 1.2. We have multiplied the measured source spectrum by these tabulated correction factors to get the source spectrum which will account the fine structure in source beam. The resultant spectrum is also plotted in Fig 1.2. Such correction changes the area under source spectrum in the neutron energy rage (0.5 – 12.0) MeV from 2471.20 to 2738.28 $n/cm^2/kW/min$, i.e. by +10.8%.

A fine structure in the source beam spectrum, caused by the water shield of reactor core, could be more precisely estimated by Monte-Carlo nowadays. However the lack of detailed and exact information about the TSR-II reactor fuel and shield prevent to do this. The latter could have substantial impact at energies below 3 MeV, where the spectra measured at several positions are notably different as seen in Fig. 1.2.

The single material presented in the input deck is a liquid oxygen. The oxygen atom density 0.0429E+24 atoms/cm^3 are taken from Report ORNL-TM-2242 [5]. The isotope fractions then were computed from elemental composition.

The spectrum of neutrons transmitted through the oxygen broomstick was computed utilzing the f4 neutron tally which provides the track length estimate over the volume of the NE-213 detector (cell 4).

The measured quantity in this benchmark is the absolute neutron energy spectra at detector position $N(E)$. To get similar response from the MCNP simulation the neutron tally has to be multiplied by normalization factor

$$fm = \int_{E1}^{E2} N_0(E)dE \left/ (1/\pi r^2) \right. ,$$

    where: $N_0(E)$ is the absolute source spectrum measured without sample,

        $E1$ = 0.5 MeV to $E2$ = 12.0 MeV are the energy integration limits,

        r = 5.75724 cm is a radius of the neutron beam cone at detector position.

For the fine structured source spectrum the integral equals 2738.28 $n/cm^2/kW/min$, thus fm = 285.139 n//kW/min. Additionally, the tally has to be divided by the energy bin widths to get an energy spectrum.

The energy resolution was reported by authors. In the MCNP deck it was represented by a Gaussian distribution with FWHM = 0.33 $\sqrt{E}$, shown as fit curve in Fig. 1.2.

The MCNP perturbation capabilities allow an estimation of the sensitivities of the transmitted neutron spectrum (benchmark response) to the nuclear reaction cross sections or other parameters of the experiment. The input deck contains an example of the perturbation cards for computing the sensitivities to the neutron cross sections with a help of 1% variation of the cross section or oxygen density.

Other details are available in the MCNP input deck as self-explaining comments.

3. Validation analysis of the ORNL oxygen broomstick with ENDF/B-VIII.0 and JEFF-3.3

The neutron transmission energy spectra were calculated by code MCNP [11] with cross section data for isotopes ^{16}O, ^{17}O and ^{18}O from libraries ENDF/B-VIII.0 [12] and JEFF-3.3 [13] (it has to be noted that JEFF-3.3 has adopted the evaluation for ^{16}O from ENDF/B-VII.1). The files were processed in the ACE format by the NJOY21 code [14] with temperature for Doppler broadening T = 90.19^{o}K = −182.96^{o}C which is a boiling point of liquid oxygen.

The calculated MCNP results for the 60" (152.4 cm) thick O-broomstick are displayed and compared with measured data in Fig. 3.1. It is seen that both ENDF/B-VIII.0 and JEFF-3.3 predict the measured yield (peak) of the 2.35 MeV neutrons practically within the experimental uncertainty ≈ 10%. However above 4 MeV, they underestimate the measured neutron transmission spectrum by 20 - 40%, the JEFF-3.3 evaluation being more preferable than ENDF /B-VIII.0.
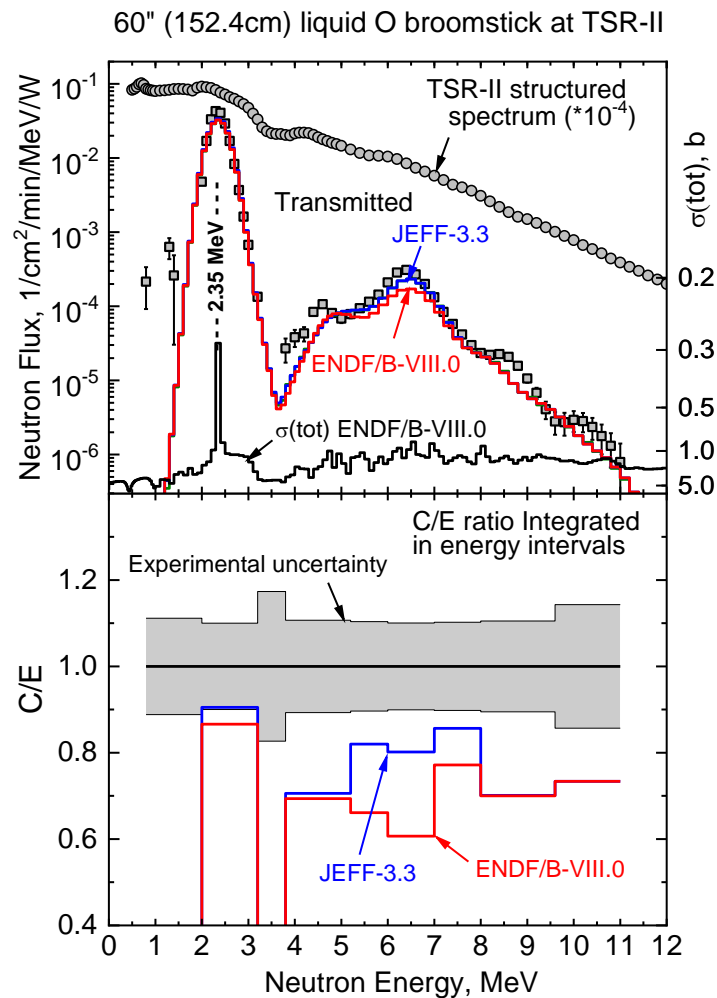

Fig. 3.1. (Top) The TSR-II source and transmitted neutron spectra for the 60" (152.4 cm) liquid Oxygen broomstick. Symbols – ORNL measurements; colour curves – MCNP transport calculations with ENDF/B-VIII.0 or JEFF-3.3; black histogram - 640-groups total cross sections for ^{16}O *(note the inverse direction of Y scale)*. (Bottom) C/E ratios integrated in the energy intervals which capture the spectrum peculiarities.

2.35 MeV transmission peak which corresponds to the cross section minimum. Fig. 3.2 shows the transmission $T(E) = N(E)/N_0(E)$ which we calculated from the measured ORNL data as a ratio of transmitted $N(E)$ and TSR-II source spectra $N_0(E)$ for the 60" liquid Oxygen broomstick in the energy

window 1 – 4 MeV. Figure also plots the MCNP transport calculation with ENDF/B-VIII.0 (the NE-213 detector energy resolution was applied) and analytically calculated transmission T (without energy resolution, but with Doppler broadening of the oxygen cross sections).

The analytic transmission was estimated in following way:

$$T(E) = exp(- n \; t \; \sigma_{tot}(E)) \qquad\qquad (1)$$

where: t – sample thickness,

n - Atom density (in case of the 60" O-broomstick n = 0.0429 1/cm-b) and

$\sigma_{tot}(E)$ – total neutron reaction cross section for elemental oxygen.

The total cross sections for the ^{16}O, ^{17}O and ^{18}O isotopes after Doppler broadening with temperature 90.19°K are also plotted in Fig. 3.2. The minimum values of the ^{16}O(n,tot) cross section in evaluated data libraries are:

- 0.1032 b at 2.351 MeV - in ENDF/B-VIII.0 and
- 0.1125 b at 2.350 MeV - in JEFF-3.3, or +9.0% larger than in ENDF/B-VIII.0.
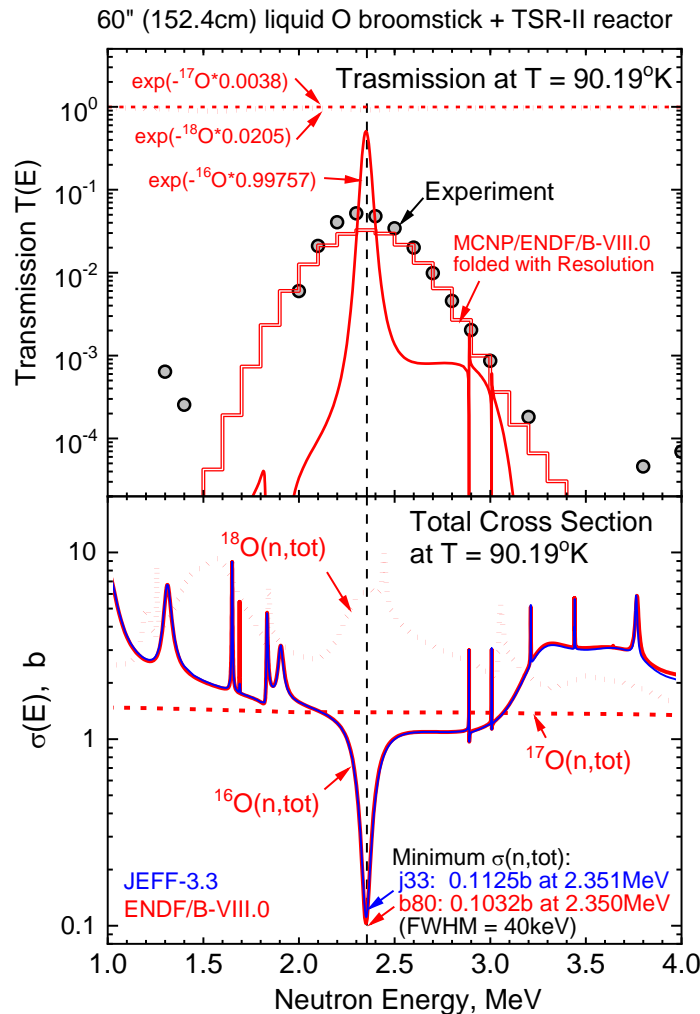

Fig. 3.2. (Top) Transmission of the neutron for the 60" (152.4 cm) liquid Oxygen broomstick. Symbols – ORNL measurement; curves – analytical (single curve) and MCNP transport calculation with ENDF/B-VIII.0 and NE-213 energy resolution (double histogram). (Bottom) Neutron total cross sections for the ^{16}O, ^{17}O and ^{18}O isotopes from ENDF/B-VIII.0 (red lines) at temperature 90.19°K. The vertical dashed line indicates the energy of local minimum for ^{16}O(n,tot).

This local minimum in the ^{16}O(n,tot) cross section at 2.35 MeV eventually defines the peak in the transmission spectrum as seen in Fig. 3.2, since $T(E)$ resulted from other isotopes ^{17}O and ^{18}O are close to unity. The negligible impact of these isotopes is explained by the absence of the (n,tot) local minima in vicinity of 2.35 MeV and by relatively small isotope abundancies: 0.038% (^{17}O) and 0.205% (^{18}O). Note that the elemental oxygen transmission is a product of $T(E)$ for three oxygen isotopes.

The 9% larger ^{16}O(n,tot) cross section minimum at 2.35 MeV from JEFF-3.3 than ENDF/B-VIII.0 causes $\approx 5\%$ lower calculated transmitted neutron yield in the $(2 - 3)$ MeV window and better agreement of this library with ORNL benchmark, as seen in Fig. 3.1.

It is worth mentioning that the energy width of the 2.35 MeV valley in the ENDF/B-VIII.0 or JEFF-3.3 cross section (FWHM = 40 keV) is substantially less than the NE-213 detector energy resolution (FWHM ≈ 500 keV). The Doppler motion at temperature 90.19°K results in the lesser broadening width FWHM ≈ 0.1 keV.

Fig. 3.3 demonstrates the <u>relative spectral contribution of the collided neutrons</u> which undergone either 1 or more than 2 collisions in the 152.4 cm long oxygen sample and reached the NE-213 detector. It is seen that at neutron energy above approximately 1.5 MeV the single or multiply scattered neutrons make an energy independent contribution at the level of 10^{-4} relatively to the uncollided neutrons.
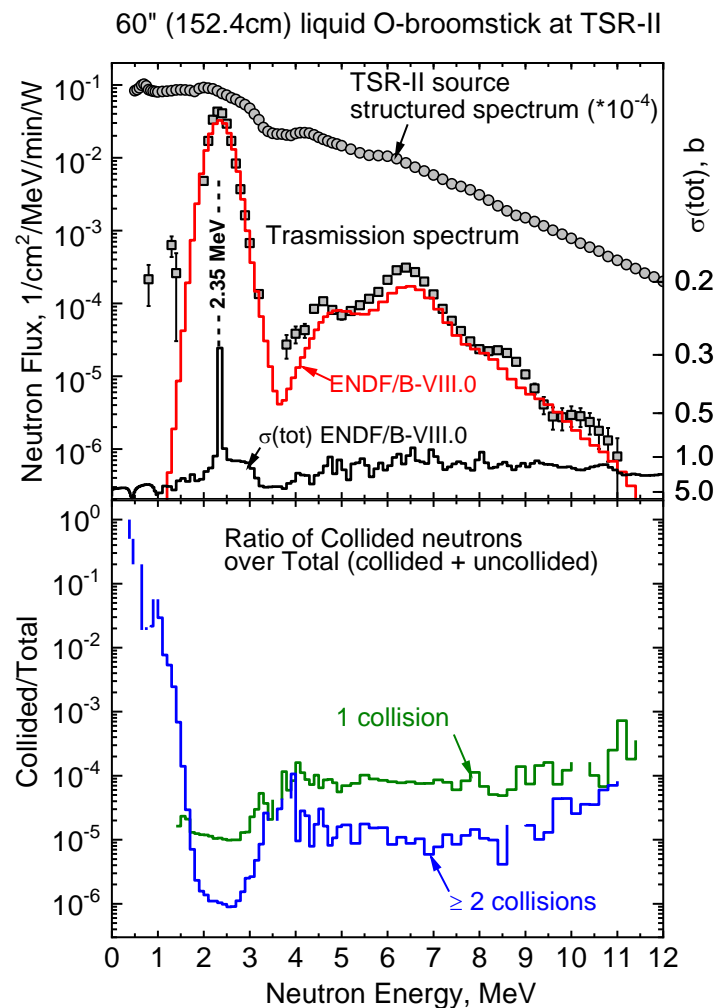

Fig. 3.3. (Top) The TSR-II source and transmitted neutron spectra for 60" (152.4 cm) liquid Oxygen broomstick: symbols – ORNL measurements; red curve – MCNP transport calculation with ENDF/B-VIII.0; black histogram – 640-groups ^{16}O(n,tot) cross section *(note the inverse direction of Y-scale)*. (Bottom) Computed ratios of collided (1 or more than 2 collisions) over the total (un- and collided) neutrons.

As it was discussed in Section 2, <u>the neutron angular divergence (or resolution) of the ORNL TSR-II Ø4"×60" oxygen broomstick experiment</u> is defined by the angle at which the NE-213 detector sees the oxygen sample of Ø4": Θ = 0.190985°, corresponding cos(Θ) = 0.999995. The probability of neutrons after the first (elastic) collision to hit the neutron detector depends on the elastic scattering angular anisotropy. The plot produced by NJOY21, Fig. 3.4, shows the angular elastic cross sections for reaction $^{16}O(n,n_{el})$ stored in ENDF/B-VIII.0.

Analytical estimation of the fraction of elastically scattered neutrons within angle subtended by sample angle Θ = 0.191° and reached detector gives $(1 - cos(\Theta)) \times \sigma_{el}(0°) / (\sigma_{el}/4\pi) \approx$ 5.E-6 $\sigma_{el}(0°) / (\sigma_{el}/4\pi) \approx$ 1.E-4. This analytical value confirms the fraction of collided neutrons ≈ 1.E-4 computed with the help of MCNP. In other words: elastic collisions will direct only 1 from 10 000 neutrons towards the neutron detector preventing others to hit it.
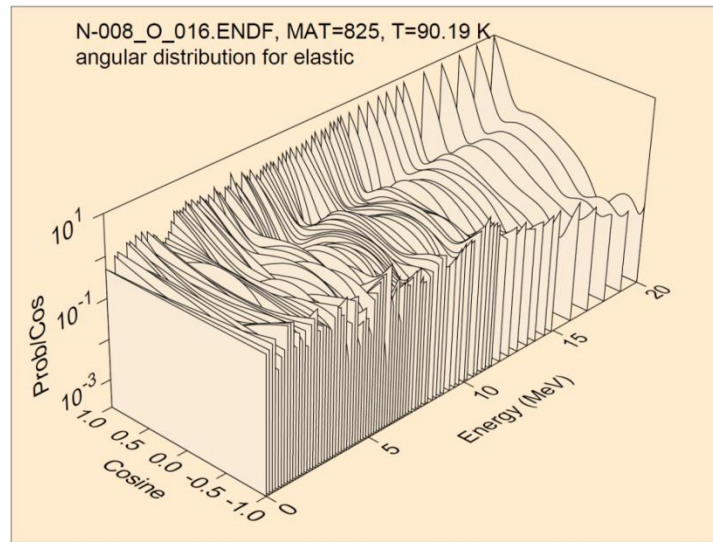

Fig. 3.4. The angular distributions of the elastically scattered neutron for reaction $^{16}O(n,n_{el})$ at neutron energies from 0 to 20 MeV. Plot is produced by NJOY21 from ENDF/B-VIII.0.

4. Sensitivity analysis of the ORNL oxygen broomstick benchmark

The sensitivity of the transmitted spectrum to the oxygen atoms density and to cross sections were computed by two ways.

(1) <u>Analytically</u>, i.e. using formula (1). Differentiation of this expression gives the sensitivity coefficient S either to the atom density n or to the total cross section $\sigma_{tot}(E)$:

$$S(E) = (\Delta T(E) / T(E)) / (\Delta n / n) = (\Delta T(E) / T(E)) / (\Delta \sigma_{tot}(E) / \sigma_{tot}(E)) = n\, t\, \sigma_{tot}(E) \qquad (2).$$

This expression proves that both sensitivities are mathematically identical. In particular it means that the variable (atom density or cross sections) with larger uncertainty will define the sensitivity of the whole benchmark.

Further derivations show that the sensitivity $S_i(E)$ to the partial neutron cross section $\sigma_i(E)$ equals the sensitivity $S(E)$ to the total cross sections $\sigma_{tot}(E)$ reduced by the corresponding cross sections ratio:

$$S_i(E) = (\Delta T(E) / T(E)) / (\Delta \sigma_i(E) / \sigma_i(E)) = n\, t\, \sigma_{tot}(E)\, \sigma_i(E) / \sigma_{tot}(E) = \sigma_i(E) / \sigma_{tot}(E)\, S(E) \quad (3).$$

Regrettably but the uncertainty of the oxygen atom concentration n in broomstick is not explicitly given by the authors of the experiment. Hence, we can only guess the minimal value of the relative uncertainty of the atom density n:

- either from the last digit given for n value $\Delta n / n = 0.0001/0.0429 = 0.2\%$,
- or from reported chemical purity of oxygen $\Delta n / n = 0.1/99.9 = 0.1\%$.

The formulas (2) – (3) do not account for the neutron detector resolution (it should be noted that the authors of the ORNL broomstick benchmarks did unfold the analytical transmission with spectrometer resolution function [4 - 7]).

(2) <u>Monte-Carlo simulation</u>, i.e. using the perturbation capabilities of the MCNP code during simulation of the oxygen broomstick experiment with all details (in particular folding with the NE-213 detector energy resolution represented by the Gaussian distribution with FWHM = 0.33 $\sqrt{E}$). In such a way the f4 neutron tally perturbations caused by small variation of the oxygen atom density n or cross sections σ_{tot}, σ_{el}, $\sigma_{(n,\alpha)}$ were computed and then the sensitivities were derived.

Fig. 4.1 shows the sensitivities to the atom density n and to the total and partial cross sections computed with help of MCNP and analytically. As seen the analytic sensitivity computed without detector energy resolution reflects the fine structure of the cross section. MCNP calculations demonstrate the numerical identity of sensitivities to n and σ_{tot}. Above 4 MeV the value of sensitivity S is around -7 to the total, ≈ -4 to the elastic and ≈ -1 to the (n,α) cross sections.
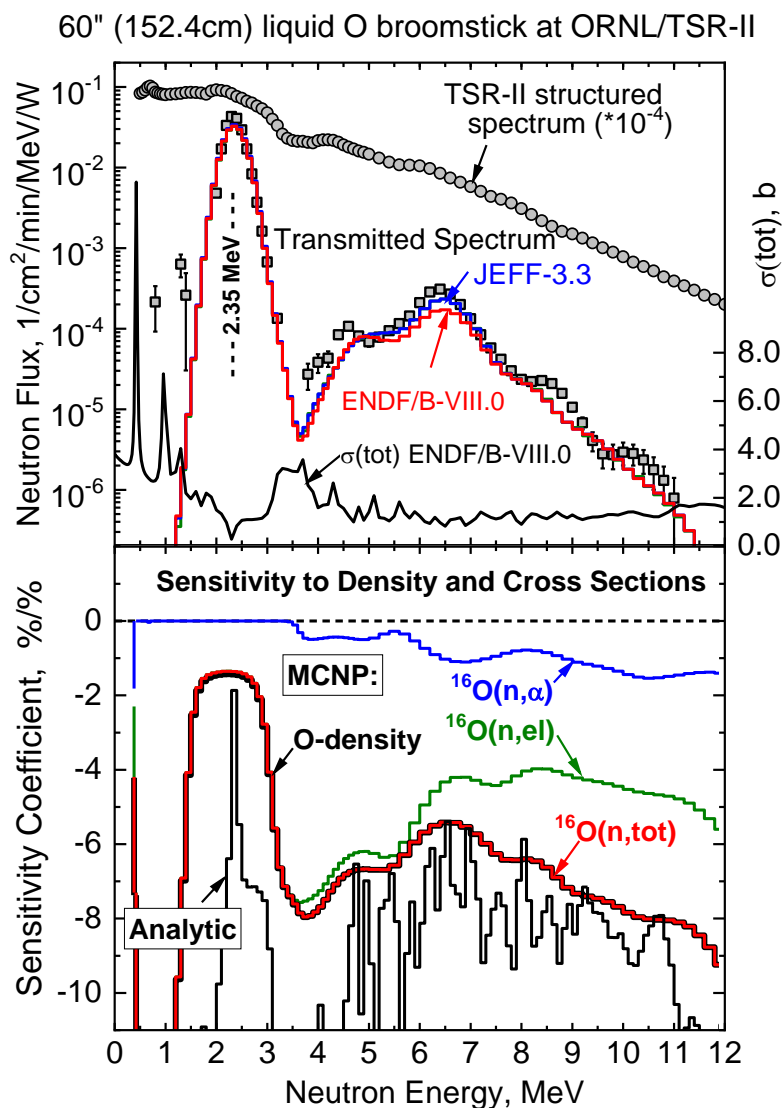

Fig. 4.1. (Top). The TSR-II source and transmitted neutron spectra for 60" (152.4 cm) liquid O-broomstick: symbols – ORNL measurements; colour curves – MCNP transport calculations with ENDF/B-VIII.0 and JEFF-3.3; black histogram – 640-groups ^{16}O(n,tot) cross section. (Bottom). Sensitivity of the neutron transmission spectra to the variation of the oxygen density, neutron total, elastic and (n,α) cross sections, calculated analytically (black histogram) or by MCNP with the ENDF/B-VIII.0 data (colour).

5. Impact of the ORNL oxygen broomstick on the (n,tot) and (n,α) cross sections

The authors of the ORNL experiment have mainly aimed to test a minima in the $^{16}O(n,tot)$ cross sections. Nowadays the problem of the discrepant experimental and evaluated data for the $^{16}O(n,\alpha)$ reaction in the neutron energy range from 4 to 8 MeV is considered as a challenge and attracts many efforts, see e.g. [22]. In this section we attempt to observe the impact of the ORNL O-broomstick neutron transmission data on the both total and (n,α) oxygen cross sections.

The primary outcome from considered transmission experiment is indeed a validation of the neutron total cross section. Thus the top part of Fig. 5.1 displays the found in EXFOR [23] the most representative experimental data [24 - 29] (it has to be noted that recent measurements of Y. Danon et al. [30], A. Junghans et al. [31] are not compiled in EXFOR yet). The vertical bars indicate the neutron energies which were computed from the excitation energies of the ^{17}O compound nucleus resonances whereas the horizontal bars graphically reflect their total widths $\Gamma \approx 2 - 150$ keV taken from ENSDF [32]. As seen in Fig. 5.1, the compound nucleus resonance widths are lower than the ORNL O-broomstick experiment energy resolution ($\approx 650 - 930$ keV). The Doppler broadening width ≈ 0.09 keV at oxygen boiling temperature 90.19°K is essentially lesser than widths of ^{17}O resonances.
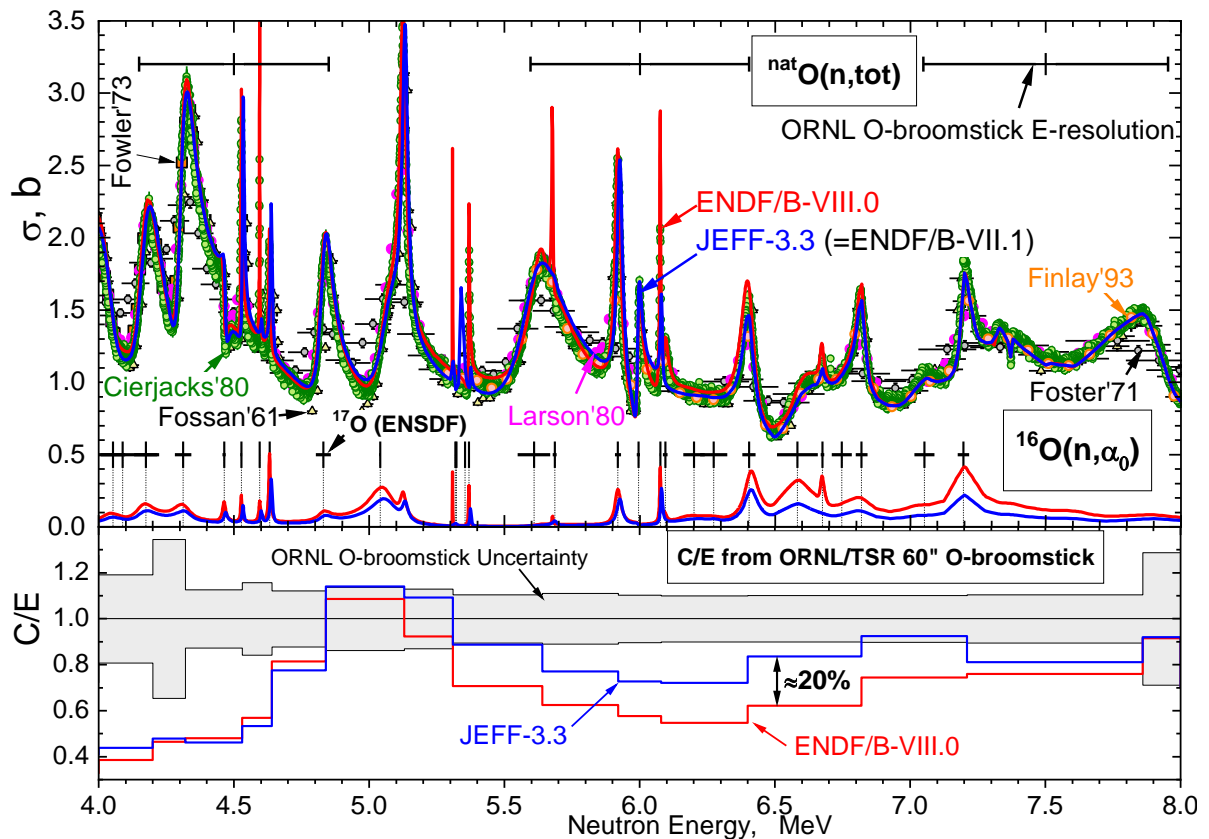

Fig. 5.1. (Top). Cross section for reaction $^{16}O(n,tot)$ and $^{16}O(n,\alpha)$: symbols – measured data [24 - 29] compiled in EXFOR, colour curves – evaluated data from ENDF/B-VIII.0 (red) and JEFF-3.3 (blue). The vertical and horizontal bars – the neutron energies and widths corresponding the ^{17}O compound excited resonances given in ENSDF. (Bottom). C/E ratios derived from analysis of the ORNL O-broomstick with ENDF/B-VIII.0 (red histogram) and JEFF-3.3 (blue) integrated in selected energy intervals. The grey corridor shows the experimental errors.

The bottom part of Fig. 5.1 depicts the C/E ratio obtained in the present Monte Carlo analysis of the ORNL/TSR-II 60” thick O-broomstick after integration in the rather wide energy intervals. The latter

were selected to capture the most prominent O(n,tot) cross section minima since transmission is sensitive to valleys whereas the resonances tend to self-shielding. Selection of group representation for C/E should also take into account the energy resolution of the NE-213 detector since it smears the fine energy structure within an energy window ≈ 0.9 MeV. The observed C/E ratio points to the better agreement (typically within $1 - 2$ experimental uncertainty) in the case of JEFFF-3.3, whereas ENDF/B-VIII.0 shows additionally $\approx 20\%$ larger underestimation between 5.3 and 7.2 MeV.

Using the calculated sensitivity of the ORNL experiment to $\sigma(n,tot) \approx - 7$ we can approximately estimate the required correction of the oxygen total cross section as:

total cross section correction $= \Delta\sigma_{tot}(E) / \sigma_{tot}(E) = (\Delta T(E)/T(E)) / S/E)) \approx 20\% / (-7) = -2.9\%.$

The $\approx 3\%$ demand of the O-broomstick benchmark to down-scale the ENDF/B-VIII.0 total cross section should be applied rather to the minima than to the maxima of cross sections. Thus, it will not cause a conflict with total cross section data well measured utilizing the thin samples. As an illustration, we refer to the measurement of S. Cierjacks et al. [27] who have reported 2 - 3% uncertainty for the total cross section. This value is generally comparable with correction stemming from the O-broomstick benchmark, moreover the latter will be applied mainly to cross section valleys.

The total cross section in the in interval 5 - 8 MeV is practically a sum of elastic scattering and (n,α) reaction. There we may consider the propagation of the observed additional 20% underestimation by ENDF/B-VIII.0 (in comparison with JEFF-3.3) to the ^{16}O(n,α) cross section using the estimated averaged sensitivity value to $\sigma(n,\alpha) \approx -1$ (see Fig. 4.1):

(n,α) cross section correction $= \Delta\sigma(n,\alpha) / \sigma(n,\alpha) \approx (\Delta T(E) / T(E)) / (-1) \approx -20\%.$

More precisely, the variation of the (n,α) cross section $\Delta\sigma_{n,\alpha}(E)$ required by the *C/E* ratio observed for the neutron transmission *T(E)* in the ORNL neutron transmission benchmark could be expressed as:

$$\Delta\sigma_{n,\alpha}(E) \equiv \sigma_{n,\alpha}(E) - \sigma_{n,\alpha}{}^{cor}(E) = \sigma_{n,\alpha}(E) / S_{n,\alpha}(E) \times (\Delta T(E) / T(E))$$
$$= \sigma_{n,\alpha}(E) / S_{n,\alpha}(E) \times (T_{Cal}(E) - T_{Exp}(E) / T_{Exp}(E) = \sigma_{n,\alpha}(E) / S_{n,\alpha}(E) \times (C/E(E) - 1) , \quad (4a)$$

where $\sigma_{n,\alpha}(E)$ and $\sigma_{n,\alpha}{}^{cor}(E)$ are the cross sections used in benchmark simulation and one resulting from required correction. To have corrected cross section this relation could be reformulated as:

$$\sigma_{n,\alpha}{}^{cor}(E) = \sigma_{n,\alpha}(E) - \sigma_{n,\alpha}(E) / S_{n,\alpha}(E) \times (C/E(E) - 1) = \sigma_{n,\alpha}(E) (1 - (C/E(E) - 1) / S_{n,\alpha}(E)). \quad (4b)$$

Fig. 5.2 collects the measured and evaluated cross sections for the ^{16}O(n,α) reaction [33 - 36] in the energy range from 5 to 8 MeV (regrettably but the data [37, 38] are not compiled in EXFOR yet). It is seen that up to 7.8 MeV the total α-particle production is essentially defined by the population only the ^{13}C ground state, i.e. by reaction ^{16}O(n,α$_0$)^{13}C in spite that the kinematic threshold for ^{16}O(n,α$_1$)^{13}C(U$_1$ = 3.089 MeV) is 5.640 MeV. This allows to additionally employ the cross section data measured for the inverse reaction ^{13}C(α,n$_{0+1}$)^{16}O [39 - 41]. The later were converted into (n,α$_0$) using the detailed balance principle [42, 43] (this particular couple ^{16}O(n,α)^{13}C and ^{13}C(α,n)^{16}O was used first time for demonstration of the detailed balance conversion option for implementation in EXFOR [44]). As seen in Fig. 5.2 the experimental data of S. Harissopulos [41] essentially disagree with other known data at E$_n$ > 6.7 MeV (E$_\alpha$ > 5.4 MeV). Recently P. Mohr has shown [45] that S. Harissopulos data has to be downscaled by up to 40% starting from α-particle energy E$_\alpha \approx 5.2$ MeV.

We use the underestimation of the ORNL/TSR-II O-broomstick neutron transmission spectra observed with ENDF/B-VIII.0 (see C/E ratio in Fig. 5.1) and sensitivity of this benchmark to the ^{16}O(n,α$_0$) cross section (see Fig. 4.1) to correct this cross section in accordance the exact relation (4). Resultant ^{16}O(n,α) cross section is depicted in the Fig. 5.2. It is seen that the feedback from the oxygen broomstick benchmark demands the decreasing of the ENDF/B-VIII.0 ^{16}O(n,α$_0$) cross section. In the neutron energy interval between 5.4 and 5.9 MeV the correction results in the diminishing of the ^{16}O(n,α) cross sections. The reason for that is thought to be extremely low values of σ(n,α). Between 5.9 and 7.7 MeV the correction is rather stable and amounts around $\approx (10 - 15)\%$.
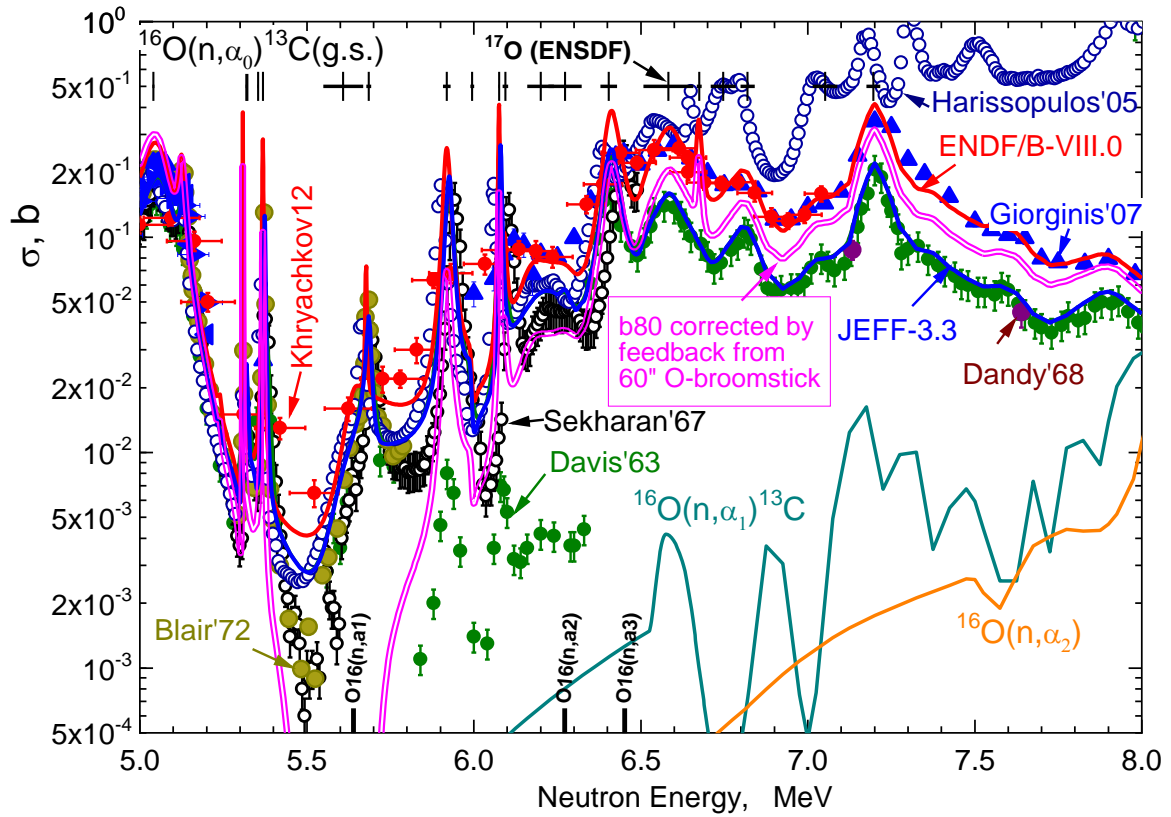
Fig. 5.2. Cross sections for $^{16}O(n,\alpha_i)$ reactions: closed symbols – direct measurements [33 - 36], open symbols - cross sections converted from the inverse reaction $^{13}C(\alpha,n_0)^{16}O$ [39 - 41]; curves – ENDF/B-VIII.0 (red) and JEFF-3.3 (blue). The vertical and horizontal bars: the neutron energies and width corresponding to the ^{17}O excited resonances from ENSDF; kinematic thresholds for reactions $^{16}O(n,\alpha_i)^{13}C(U_i)$. The ENDF/B-VIII.0 $^{16}O(n,\alpha_0)$ cross section corrected for the feedback from the ORNL 60" O–broomstick transmission experiment is shown by the double pink curve.

6. Cross-checking of the ORNL 60" O-broomstick impact on $^{16}O(n,\alpha)^{13}C$ by the $^{nat}C(\alpha,n)$ TTY

As an additional check of the correction for the $^{16}O(n,\alpha)^{13}C$ cross section in the neutron energy range 6 - 8 MeV, which was derived from the validation analysis of the ORNL 60" O-broomstick, we has computed the neutron yield from the carbon thick target and compared it with the existing measured data. As it was shown recently [46, 47], the carbon (α,n) thick target data are rather consistent and could be used to fix the discrepant $^{16}O(n,\alpha)^{13}C$ cross section measurements.

There are known four experiments where neutron TTY from the elemental carbon (reactor graphite) was measured at α-particle energy E_α varying between 2 and 8 MeV [48 - 51], see Fig. 6.1. It should be underline that the data of R. Macklin and J. Gibbons [48] plotted in this figure were reduced by factor of 10 above 5 MeV and by factor 5 at lower energies as was recommended by J.K. Bair [52]. Thus, practically there is no one reliable experiment below ≈ 4 MeV (E. Ramström et al. [53] have measured the neutron yield of the $^{13}C(\alpha,n)^{16}O$ reaction in the energy range 0.60 - 1.15 MeV, which is extremely low for present analysis).

Due to high kinematic threshold 11.338 MeV of the (α,n) reaction on the main isotope ^{12}C, the neutrons are generated only by $^{13}C(\alpha,n)^{16}O$ at considered α-particle energies. The neutron TTY was calculated by the *d-Active* code [54]. The elemental carbon was supposed to be the reactor graphite (which was used as a target in experiments) with density 1.70 g/cm^3. The natural abundance of ^{13}C in graphite varies

between 1.0608 and 1.1124% [55]. An averaging brings the value 1.0866% with relative uncertainty ± 2.4%, that was used in our TTY calculations. The α-particle energy losses were taken from the ASTAR code at the NIST web-site [56]. The $^{16}O(n,\alpha_0)^{13}C$(g.s.) cross sections from ENDF/B-VIII.0 and JEFF-3.3 were transformed into $^{13}C(\alpha,n_0)^{16}O$(g.s.) by own code and then were used for computing neutron TTY.
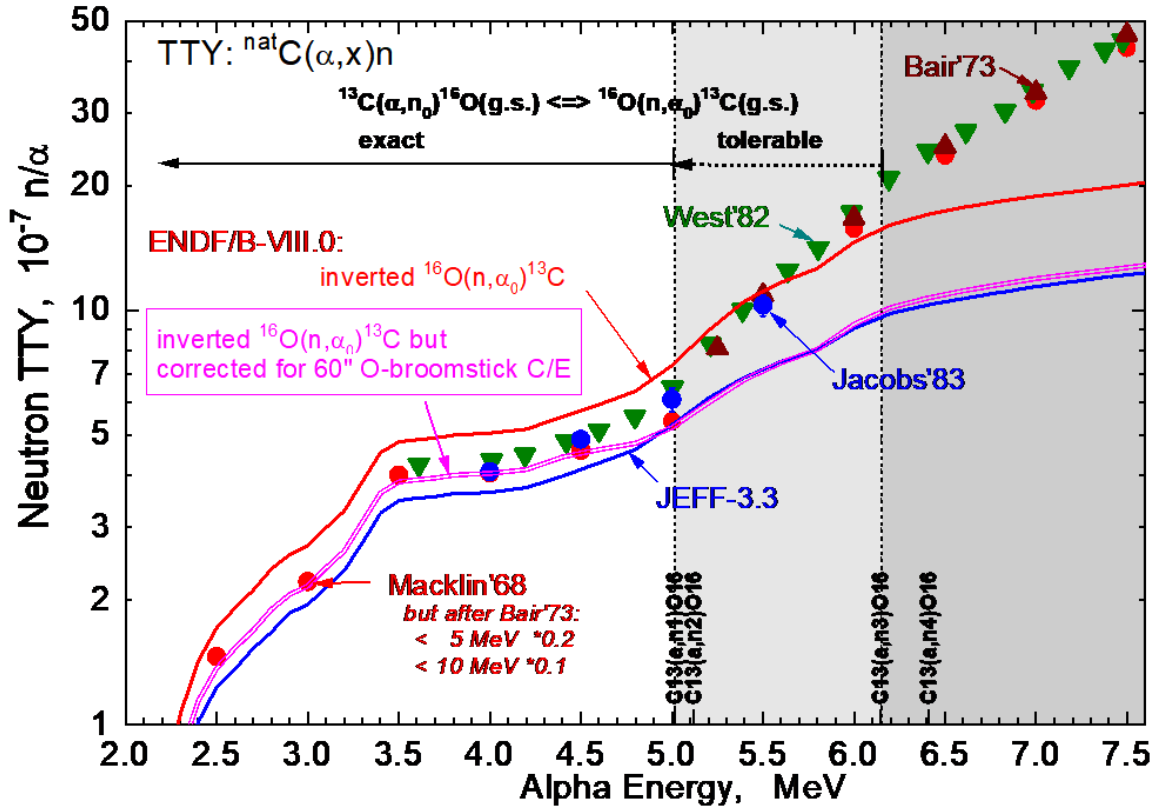

Fig. 6.1. The total neutron yield versus incident α-particle energy: symbols – experimental data [48 - 51], curves – calculations with $^{16}O(n,\alpha_0)^{13}C$ reaction cross section from ENDF/B-VIII.0 (red) and JEFF-3.3 (blue) converted into $^{13}C(\alpha,n)^{16}O$ using the detailed balance principle. The threshold for the channels $^{13}C(\alpha,n_i)^{16}O(U_i)$ are indicated by the vertical bars and notations. The TTY computed with the ENDF/B-VIII.0 $^{16}O(n,\alpha_0)^{13}C$ cross section corrected for the validation feedback from the ORNL 60" O–broomstick transmission experiment is shown by the double pink curve.

The calculated results are compared with measured ones in Fig. 6.1. Kinematically the comparison is correct in the α-particle energy range from zero (population of the ground state of ^{13}C) up to 5.014 MeV (excitation of the 1st level $U_1 = 6.049$ MeV in ^{13}C). Probably, we can extend this interval up to 6.149 MeV (excitation of the 3rd level $U_3 = 6.917$ MeV in ^{13}C), since the cross sections for $^{16}O(n,\alpha_1)^{13}C$(6.049 MeV) and $^{16}O(n,\alpha_2)^{13}C$(6.130 MeV) are still relative small as seen in Fig. 5.2. Above $E_\alpha \approx 6$ MeV all opened $^{13}C(\alpha,n_i)^{16}O(U_i)$ partial channels should be added.

As seen in Fig. 6.1, at alphas energies below 5 MeV the calculation with $^{16}O(n,\alpha_0)^{13}C$(g.s.) from the ENDF/B-VIII.0 evaluation overestimates the thick neutron target yield induced by α-particles whereas JEFF-3.3 underestimates. However, the $^{16}O(n,\alpha_0)^{13}C$(g.s.) from ENDF/B-VIII.0 after correction by deviations observed in the analysis of the ORNL/TSR-II 60" liquid broomstick (see C/E ratio as a function of the neutron energy in Fig. 5.1) do agree better.

Summary

The existing entry NEA-1517/59 (SDT2) of the SINBAD database was upgraded. This entry has comprised the measured neutron spectra from the TSR-II reactor source and after transmittion through the 60" thick liquid oxygen broomstick. The experiment was carried at Oak Ridge National Laboratory and results were published in period 1968 - 1972.

The actual upgrade additionally includes the MCNP model input deck assembled for this experiment and the present evaluation report which describes the necessary details of experiment and validation analysis.

Communication with RSICC at ORNL was undertaken to seek the numerical data for the neutron spectra transmitted through O-broomsticks of the 24" and 36" (and probably 72") length, but without success.

From the analysis of existing experimental data for the ORNL 60" thick O-broomstick benchmark and performed Monte Carlo or analytical simulations the following conclusions were derived.

Completeness and quality of experimental data:

- The neutron source spectrum, i.e. ones emerging from TSR-II reactor, was measured by the scintillation detector with energy resolution $\approx 10\%$. Such insufficient resolution has not allowed to the authors of experiment to observe the fine energy structure caused by transmission through the water shield of the TSR-II reactor core. They have recommended to correct the spectrum incident on O-broomstick by the energy oscillating function reaching up to 40%. To increase the benchmark representativeness for the oxygen cross sections validation, the transmission of the core neutron through the water shield could probably be re-simulated with higher precision nowadays.

- The spectrum of neutrons transmitted through 60" thick O-broomstick is given as upper and lower limits resulting from the unfolding of the recoil pulse distribution registered by the NE-213 detector. The negative values and more than 100% difference between upper and lower limits restrict the usage experimental data to the energy intervals (2.0 - 3.2) MeV and (3.8 - 8.0) MeV.

- The uncertainty of the atom density in the liquid oxygen broomstick and chemical admixtures are not given, that forced us to guess these values.

Analysis and validation outcome:

- The fraction of the collided and uncollided neutrons was found to be at level $\approx 10^{-4}$. This was confirmed analytically (using the angle subtended by detector and angular distribution of elastically scattered neutrons) and also directly by MCNP using its capability to bin the detector response over the number of collisions.

- Due to such negligible contribution of the collided neutrons the analytical and Monte Carlo analysis deliver practically identical results. However, the use of MCNP makes easier to imply detector resolution, calculate contribution of collided neutrons, sensitivity etc.

- Sensitivity of 60" O-benchmark to the oxygen total cross section varies between -2 and -8 reaching maximum at ^{16}O(n,tot) resonance peaks (even the larger value up to -10 could be reached if the facility energy resolution will be improved).

- Since sensitivity to the oxygen total cross section and to the broomstick atom density is identical, it is impossible to get the relative uncertainty for derived σ(n,tot) better than an error of the oxygen atom density, i.e. $\approx 0.2\%$ as we assumed for this experiment.

- The Monte Carlo simulation of the 60" O-broomstick produces an evidence that the ^{16}O(n,tot) cross section from JEFF-3.3 (which is identical to ENDF/B-VII.1) behaves better than ones from ENDF/B-VIII.0.

- Propagation of the underestimation observed for the 60" O-broomstick neuron transmission with ENDF/B-VIII.0 data to the ^{16}O(n,α) cross section demands its decreasing by $\approx (10 - 15)\%$ between 5.5 and 8.0 MeV.

- Such outcome from this validation benchmark is shown do agree with the thick carbon target neutron yield induced by α-particles with energies up to 5 - 6 MeV.

Acknowledgment

References

1. "Shielding Integral Benchmark Archive and Database (SINBAD)", available on the NEA Data Bank web-site: https://www.oecd-nea.org/science/wprs/shielding/
2. "International Criticality Safety Benchmark Evaluation Project (ICSBEP)", available on NEA Data Bank web-site https://www.oecd-nea.org/science/wpncs/icsbep/
3. Subgroup 47 "Use of Shielding Integral Benchmark Archive and Database for Nuclear Data Validation" of the Working Party on International Nuclear Data Evaluation Co-operation, Nuclear Energy Agency, Paris.
4. C.E. Clifford, E.A. Straker, F.J. Muckenthaler et al., "Measurements of the Spectra of Uncollided Fission Neutrons Transmitted Through Thick Samples of Nitrogen, Oxygen, Carbon, and Lead: Investigation of the Minimum Total Cross Sections", Nucl. Sci. Eng. 27 (1967) 299.
5. E.A. Straker, "Experimental Evaluation of Minima in the Total Neutron Cross Sections of Several Shielding Materials", Report ORNL-TM-2242, Oak Ridge, June 1968.
6. E.A. Straker, F.J. Muckenthaler, J.L. Hull et al., "Experimental Evaluation of Minima in the Total Neutron Cross Sections', Report ORNL-4134, p. 57, Oak Ridge, August 1967.
7. R.E. Maerker, "SDT2. Oxygen Broomstick Experiment-An Experimental Check of Neutron Total Cross Sections", Report ORNL-TM-3868 (revised), Oak Ridge, September 1972.
8. R.E. Maerker and F.J. Muckenthaler, "The absolute neutron spectrum emerging through a 15-1/4 in. collimator from the TSR-II reactor at the Tower Shielding Facility", Report ORNL-TM-4010, Oak Ridge, 1972.
9. SINBAD collection: „SDT2. Oxygen Broomstick Experiment - An Experimental Check of Neutron Total Cross Sections - 1968 ", Abstract NEA-1517/59, NEA Data Bank,
10. SINBAD collection: „SDT1. Iron Broomstick Experiment - An Experimental Check of Neutron Total Cross Sections - 1968", SINBAD Abstract NEA-1517/58, "SDT3. Nitrogen Broomstick Experiment", Abstract NEA-1517/60 , SDT11. Neutron Transport Through Iron and Stainless Steel, Part I – 1974", Abstract NEA-1517/62 .
11. MCNP - a general-purpose Monte Carlo N-Particle code: https://mcnp.lanl.gov/ .
12. D.A. Brown, M.B. Chadwick, R. Capote et al., "ENDF/B-VIII.0: The 8th Major Release of the Nuclear Reaction Data Library with CIELO-project Cross Sections, New Standards and Thermal Scattering Data", Nuclear Data Sheets 148 (2018) 1.
13. A.J.M. Plompen, O. Cabellos, C. De Saint Jean et al., "The Joint Evaluated Fission and Fusion Nuclear Data Library", The European Physical Journal A56 (2020) 181.
14. "NJOY21 - NJOY for the 21st Century"; available on: https://www.njoy21.io/NJOY21/ .
15. S. Simakov, U. Fischer, "Remarks from use of SINBAD", Meeting of SG47 "Use of Shielding Integral Benchmark Archive and Database for Nuclear Data Validation", 24 June 2019, NEA Headquarters, Paris.
16. S. Simakov, U. Fischer, "KIT contribution to SG-47: progress since June 2019", Meeting of SG47 "Use of Shielding Integral Benchmark Archive and Database for Nuclear Data Validation", WebEx meeting, 12 May 2020.
17. S. Simakov, U. Fischer, "SINBAD new/updated Entries: KFK γ-ray leakage and ORNL O-broomstick neutron transmission", Meeting of SG47 "Use of Shielding Integral Benchmark

Archive and Database for Nuclear Data Validation", WebEx meeting, 11 May 2021, NEA Headquarters, Paris.

18. M. Kostal, E. Losa, M. Schulc et al., "Validation of IRDFF-II library in VR-1 reactor field using thin targets", Annals of Nuclear Energy 158 (2021) 108268.

19. C.E. Clifford, F.J. Muckenthaler et al., "Fast reactor experimental shielding progress report January 1974", Report ORNL-TM-4592, Oak Ridge, 1974.

20. R.E. Maerker, "SDT1. Iron Broomstick Experiment - An Experimental Check of Neutron Total Cross Sections", Report ORNL-TM-3867 (revised), Oak Ridge, September 1972.

21. R. Burrus, "Utilization of A Priori Information in the Statistical Interpretation of Measured Distributions", Report ORNL-3743, Oak Ridge, 1964.

22. M.B. Chadwick, R. Capote, A. Trkov et al., "CIELO Collaboration Summary Results: International Evaluations of Neutron Reactions on Uranium, Plutonium, Iron, Oxygen and Hydrogen", Nuclear Data Sheets 148 (2018) 189.

23. N. Otuka, E. Dupont, V. Semkova et al., "Towards a More Complete and Accurate Experimental Nuclear Reaction Data Library (EXFOR): International collaboration between Nuclear Reaction Data Centres (NRDC)", Nuclear Data Sheets 120 (2014) 272.

24. D.B. Fossan, R.L. Walter et al., "Neutron Total Cross Sections of Be, B^{10},B, C, and O", Phys. Rev. 123 (1961) 209.

25. D.G. Foster and D. Glasgow, "Neutron Total Cross Sections, 2.5 - 15 MeV. I. Experimental ", Phys. Rev. C8 (1971) 576.

26. J.L. Fowler, C.H. Johnson, R.M. Feezel, "Level Structure of ^{17}O from Neutron Total Cross Sections", Phys. Rev. C8 (1973) 545.

27. S. Cierjacks, F. Hinterberger et al., "High precision time-of-flight measurements of neutron resonance energies in carbon and oxygen between 3 and 30 MeV", Nucl. Instr. Meth. 169 (1980) 185.

28. D.C. Larson, J.A. Harvey, N.W. Hill, "Measurement of neutron total cross sections at ORELA to 80 MeV", Proc. of Symp. on Neutron Cross Sections 10 - 50 MeV, Brookhaven 1980, p. 277.

29. R.W. Finlay, W.P. Abfalterer, G. Fink et al., " Neutron total cross sections at intermediate energies", Phys. Rev. C47 (1993) 237.

30. Y. Danon, E. Blain, A. Daskalakis et al. "Measurement of total cross section of water and O-16 in the MeV energy range", Proc. of AccApp '15, Washington, DC, Nov 2015, p. 345.

31. A. Junghans, R. Beyer, J. Claußner et al. "Neutron transmission measurements at nELBE", EPJ Web of Conf. 239, 01006 (2020).

32. Evaluated Nuclear Structure Data File (ENSDF); data on: https://www.nndc.bnl.gov/ensdf/ .

33. E.A. Davis, T.W. Bonner, D.W. Worley, R.Bass, "Disintegration of O^{16} and C^{12} by fast neutrons", Nucl. Phys. 48 (963) 169.

34. D. Dandy, J.L. Wankling, C.J. Parnell, "The Cross Section for the O-16(n,a) reaction for neutron energies in the range 7 to 12 MeV", Report AWRE 60/68 (1968), Aldermaston, UK.

35. G. Giorginis, V. Khryachkov, V. Corcalciuc, M. Kievets, "The cross section of the 16O(n,a)13C reaction in the MeV energy range", Proc. Conf. on Nucl. Data for Sci. and Techn. (Nice 2007), vol. 1, p. 525 (2007).

36. V.A. Khryachkov, I.P. Bondarenko, B.D. Kuzminov et al. "(n,α) reactions cross section research at IPPE", EPJ Web of Conferences 21 (2012) 03005.

37. M. Febbraro, R.J. deBoer, S.D. Pain et al., "New ^{13}C(α,n)^{16}O Cross Section with Implications for Neutrino Mixing and Geoneutrino Measurements", Phys. Rev. Lett 125 (2020) 062501.

38. S. Urlass, R. Beyer et al., "Measurement of the ^{16}O(n,α)^{13}C cross section using a Double Frisch Grid Ionization Chamber", EPJ Web of Conferences 239 (2020) 01030.

39. J.K. Bair and F.X. Haas, "Total Neutron Yield from the Reactions ^{13}C(α,n)^{16}O and ^{17,18}O(α,n)^{17,18}Ne", Phys. Rev. C7 (1973) 1356.

40. K.K. Sekharan, A.S. Diviata, M.K. Mehta et al., "^{13}C(α,n)^{16}0 Reaction Cross Section between 1.95 and 5.57 MeV", Phys. Rev. 156 (1967) 1187.

41. S. Harissopulos, H.W. Becker, J.W. Hammer et al., "Cross section of the ^{13}C(α,n)^{16}O reaction: A background for the measurement of geo-neutrinos", Phys. Rev. C72 (2005) 062801.

42. R.G. Sachs, "Nuclear Theory", Cambridge, MA, Addison-Wesley, 1953, p. 141.

43. J.M. Blatt and V.F. Weisskopf, "Theoretical Nuclear Physics", Springer-Verlag, New York Heidelberg Berlin, 1979.

44. S.P. Simakov, R. Forrest, N. Otsuka, V. Semkova, V. Zerkin, "EXFOR for CIELO project: $^{16}O(n,\alpha)^{13}C$ and $^{13}C(\alpha,n)^{16}O$ data", Technical Meeting on Int. Network of Nuclear Reaction Data Centres (NRDC), 6 – 9 May 2014, Smolenice, Slovakia, https://www-nds.iaea.org/nrdc/nrdc_2014/present/simakov3.pdf .

45. P. Mohr, "Revised cross section of the 13C(α, n)16O reaction between 5 and 8 MeV", Phys. Rev. C97 (2018) 064613.

46. M.T. Pigni and S. Croft, "Consistency of 16O(n, α) cross sections ", Phys. Rev C102 (2002) 014618.

47. A. Plompen, "$^{16}O(n,\alpha)$ database. Recommended normalization and new evaluation, final issue", JEFDOC-2034, JEFF WebEx Meetings, 29 Apr 2021, NEA Headquarters, Paris.

48. R.L. Macklin and J.H. Gibbons, "Absolute Neutron Yields from Thick Target $^{nat}C(\alpha,n)$", Nucl. Sci. Eng. 31 (1968) 343.

49. J.K. Bair, "Absolute Neutron Yields from Alpha-Particle Interaction with Thick Targets of Natural Carbon", Nucl. Sci. Eng. 51 (1973) 83.

50. D. West and A.C. Sherwood, "Measurements of thick target (a,n) yields from light elements", Annals of Nuclear Energy 9 (1982) 551.

51. G.J.H. Jacobs and H. Liskien, "Energy spectra of neutrons produced by α-particles in thick targets of light elements", Annals of Nuclear. Energy 10 (1983) 541.

52. J.K. Bair and J. Gomez del Campo, "Absolute Neutron Yields from Alpha-Particle Interaction with Thick Targets of Natural Carbon", Nucl. Sci. Eng. 71 (1973) 83.

53. E. Ramström and T. Wiedling, "The reaction rate of the $^{13}C(\alpha,n)^{16}O$ process", The Astrophysical Journal 211 (1977) 223.

54. S. Simakov, U. Fischer, A. Konobeyev, "Status and benchmarking of the deuteron induced Tritium and Beryllium-7 production cross sections in Lithium", KIT Scientific Working Papers 147, Karlsruhe, June 2020.

55. Commission on Isotopic Abundances and Atomic Weights (CIAAW), web address: https://www.ciaaw.org/.

56. ASTAR - stooping power and ranging tables for helium ions, National Institute of Standards and Technology, web address: https://physics.nist.gov/PhysRefData/Star/Text/ASTAR.html